RESEARCH PAPER

Plant Signaling & Behavior 9:10, e972887; November 1, 2014; Published with license by Taylor & Francis Group, LLC

An analytical model of memristors in plants

Vladislav S Markin[1,*], Alexander G Volkov[2,*], and Leon Chua[3]

[1]Department of Neurology; University of Texas, Southwestern Medical Center; Dallas, TX USA; [2]Department of Chemistry and Biochemistry; Oakwood University; Huntsville, AL USA; [3]Department of Electrical Engineering and Computer Sciences; University of California, Berkeley; Berkeley CA USA

Keywords: *Aloe vera*, Bioelectrochemistry, cyclic voltammetry, electrophysiology, ion channel, memristor, *Mimosa pudica*, signal transduction

Abbreviations: *C*, capacitance; *DAQ*, data acquisition; *G*, meminductance; *PXI*, PCI eXtensions for Instrumentation; *I*, electrical current; *t*, time; τ, delay time; TEACl, tetraethylammonium chloride; *V*, voltage; V_{FG}, voltage of a function generator; *Vp*, voltage between electrodes in plants; V_R, voltage on resistor *R*.

The memristor, a resistor with memory, was postulated by Chua in 1971 and the first solid-state memristor was built in 2008. Recently, we found memristors *in vivo* in plants. Here we propose a simple analytical model of 2 types of memristors that can be found within plants. The electrostimulation of plants by bipolar periodic waves induces electrical responses in the *Aloe vera* and *Mimosa pudica* with fingerprints of memristors. Memristive properties of the *Aloe vera* and *Mimosa pudica* are linked to the properties of voltage gated K^+ ion channels. The potassium channel blocker TEACl transform plant memristors to conventional resistors. The analytical model of a memristor with a capacitor connected in parallel exhibits different characteristic behavior at low and high frequency of applied voltage, which is the same as experimental data obtained by cyclic voltammetry *in vivo*.

Introduction

The concept of memristor, a resistor with memory, as the fourth basic element of electric circuitry was introduced by Leon Chua[1] in 1971. During the last decade, different memristors were developed as solid state semiconductor devices, polymers and modified electrodes.[2-10] Theoretical analysis shows the existence of memristors in neural networks, voltage gated channels, synapses and in the brain.[11-14] Analysis of the Hodgkin-Huxley axon model shows that voltage gated channels can be identified as a potassium ion-channel memristor and a sodium ion-channel memristor.[11-14] Plants have voltage gated K^+ channels and it would be interesting to investigate the possible presence of memristors in plants. A memristor is a nonlinear circuit element because its current-voltage characteristic is similar to that of a Lissajous pattern. No combination of nonlinear resistors, capacitors and inductors can reproduce this Lissajous behavior of a memristor.[4,10]

The pinched hysteresis loop of memory elements, when subject to a periodic stimulus, can be self crossing (type I memristor) or not (type II memristor).[4,10] We found that the electrostimulation of plants by bipolar periodic sinusoidal or triangle waves induces electrical responses in the Venus flytrap, *Mimosa pudica* and *Aloe vera* with fingerprints of memristors of type I or type II.[15] Memristive properties of the Venus flytrap, *Aloe vera* and *Mimosa pudica* are linked to the properties of voltage gated K^+ ion channels. The potassium channel blocker TEACl transform plant memristors to conventional resistors.[15] In some plants such as *Arabidopsis thaliana*, there are 9 Shaker channels, 5 two-pore K^+ (TPK) channels and a single IRK-like K^+ channel. All Shaker-like channels could be localized to the plasma membrane.[16-18] Electrical circuits in plants operate over large distances. Electrical signals in plants can propagate along the electroconductive plasma membrane on long distances in plasmodesmata and on short distances in conductive bundles. The recently observed response of a number of plants to external periodical signals revealed the typical fingerprints of memristors.[15] However, the mechanism of this response is unknown. To elucidate this mechanism, we propose here simple tentative analytical models of a memristor and a memristor with a capacitor connected in parallel.

There are many mathematical models of solid semiconductor memristors in literature.[4,10,19-24] They can be divided in 3 groups: linear, nonlinear, and exponential models.[16-25] Chua et al.[11,12] and Adhikari et al.[10] found that a memristor has 3 characteristic fingerprints: "When driven by a bipolar periodic signal the device must exhibit a pinched hysteresis loop in the voltage-current plane, assuming the response is periodic; starting from some critical frequency, the hysteresis lobe area should decrease monotonically as the excitation frequency increases; the pinched hysteresis loop should shrink to a single-valued function when the frequency tends to infinity." Voltage gated ion channels

*Correspondence to: Vladislav S Markin; Email: markina@swbell.net; Alexander G Volkov; Email: agvolkov@yahoo.com
Submitted: 07/13/2014; Revised: 07/14/2014; Accepted: 07/23/2014
http://dx.doi.org/10.4161/15592316.2014.972887

in biological tissue are located in membranes, which have capacitance connected in parallel to transmembrane organized ion channels. We found that in the Venus flytrap, *Mimosa pudica* and *Aloe vera* the pinched hysteresis loop does not shrink to a single-valued function when the frequency is very high.[15]

The main goal of this article is to develop analytical models of 2 types of memristors and the effects of a plant tissue capacitance on the memristive properties of plant and to compare theoretical results with our experimental data obtained by cyclic voltammetry *in vivo*.

Results

Theoretical

Leon Chua in his 1971 paper[1] defined an ideal memristor and recently he introduced a generic memristor defined by state-dependent Ohm's law:

$$i = G(x)V \tag{1}$$

and State Equation:

$$dx/dt = f(x, V) \tag{2}$$

where G(x) is called the "memductance," whose unit is Siemens, defined as the reciprocal of the "memristance" in Ohms:

$$R(x) = 1/G(x) \tag{3}$$

The above "generic memristor" shares the same properties as the ideal memristor, with the exception that the state variable "x" is not the "charge" q as before.

Here we analyze the properties of generic memristor in a simple analytical model. If we identify

$$x = R \tag{4}$$

then the associated generic memristor Equations (1) and (2) assume the special form:

$$i = [1/R]V \tag{5}$$

$$\mathrm{d}R/\mathrm{d}t = f(R, V) \tag{6}$$

Therefore we analyze the voltage - controlled memristor with memductance given by

$$G(\mathrm{x}) = 1/R \tag{7}$$

where the dynamics of the state variable R obeys the state Equation (6).

Voltage and time dependent resistor. The basic property of memristor behavior reflects the idea that its resistance is voltage and time dependent, so when external voltage changes the resistance also changes but follows the voltage with some delay. We shall investigate this idea in a simple analytical approach.

Let us consider a resistor R_m, which varies with potential difference $V(t)$ (**Fig. 1**). At constant V, the resistance is constant and equal to

$$R_{\mathrm{const}}(V) = h(V)R_0 \tag{8}$$

obtained by equating (2) to zero and solving for x = R:

$$\mathrm{d}x/\mathrm{d}t = f(\mathrm{x}, V) = 0,$$

to obtain the DC memristance

$$\mathrm{x}(V) = h(V)R_0$$

where we define $h(V)$ and R_0 such that

$$h(0) = 1 \tag{9}$$

(normalization assumption) and R_0 is a constant (steady state or DC) resistance corresponding to voltage $V = 0$. It follows that the DC resistance (when V is constant) is given by Eq. (8). When potential changes, the resistance follows these changes with a certain characteristic delay time τ. This process can be described by equation

$$\frac{dR}{dt} = -\frac{R - R_{\mathrm{const}}(V)}{\tau} \tag{10}$$

It means that resistance relaxes to the stationary value $R_{\mathrm{const}}(V) = f(V)R_0$ corresponding to the current value of potential V. The solution of this equation is

$$R(t) = \exp\left(-\frac{t}{\tau}\right)\left\{\frac{R_0}{\tau}\int_0^t h[V(\theta)]\exp\left(\frac{\theta}{\tau}\right)d\theta + A\right\} \tag{11}$$

where A is a constant of integration. Let us consider periodically changing voltage $V(t)$ with period T applied to this resistor. The resistance $R(t)$ will start changing but after a number of cycles (strictly speaking at t = infinity) it will come to periodic steady-state and $R(t)$ will cycle with the same period T. So, in a periodic steady state the solution is

$$R(t) = R(t + T) \tag{12}$$

If one takes $t = 0$, then

$$R(0) = R(T), \tag{13}$$

which gives equation for constant of integration A:

$$A = \exp\left(-\frac{T}{\tau}\right) * \left\{\frac{R_0}{\tau}\int_0^T h[V(\theta)]\exp\left(\frac{\theta}{\tau}\right)d\theta + A\right\} \tag{14}$$

It can be solved as

$$A = \frac{\frac{R_0}{\tau}\int_0^T h[V(\theta)]\exp\left(\frac{\theta}{\tau}\right)d\theta}{\exp\left(\frac{T}{\tau}\right)-1} \tag{15}$$

The electrical current through this resistor $i_m(t)$ also changes with time in a periodical manner:

$$i_m(t) = \frac{V(t)}{R(t)} = \frac{\exp\left(\frac{t}{\tau}\right)V(t)}{\frac{R_0}{\tau}\int_0^t h[V(\theta)]\exp\left(\frac{\theta}{\tau}\right)d\theta + A} \tag{16}$$

One can notice that if the resistance does not depend on voltage, meaning that $h(V) = 1$, then Equation (9) transforms into familiar Ohm's law: $i(t) = V(t)/R_0$.

Capacitor in parallel with memristor. In real measurements with plants we do not have pure memristors but a more complicated circuit with other basic elements. In our experiments we have the reason expect the presence of additional resistance and capacitor. So, we consider the circuit where the memristor R_m is connected in parallel with capacitor C plus resistor R_2 (**Fig. 1**). This additional circuit can be described by the following equations

$$\begin{aligned} V(t) &= V_{R2} + V_C, i_{R2} = \frac{V_{R2}}{R_2} = i_C = C\frac{dV_C}{dt}, \frac{V_{R2}}{R_2} \\ &= C\frac{dV_C}{dt}, \frac{V(t)-V_C}{R_2} = C\frac{dV_C}{dt}. \end{aligned} \tag{17}$$

This new branch can be characterized by parameter of time

$$\xi = R_2 C \tag{18}$$

The main equation

$$\frac{dV_C}{dt} + \frac{1}{\xi}V_C = \frac{1}{\xi}V(t) \tag{19}$$

can be solved to give

$$V_C(t) = \exp\left(-\frac{t}{\xi}\right)\left\{\frac{1}{\xi}\int_0^t V(\theta)\exp\left(\frac{\theta}{\xi}\right)dt + B\right\} \tag{20}$$

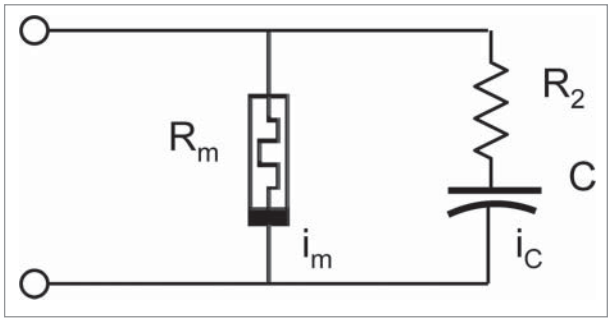

Figure 1. Electrical circuit.

where B is a constant of integration. With periodic signal $V(t) = V_0 \sin\omega t$ the equation becomes

$$V_C(t) = \exp\left(-\frac{t}{\xi}\right)\left\{\frac{1}{\xi}\int_0^t V_0 \sin\omega\theta \exp\left(\frac{\theta}{\xi}\right)d\theta + B\right\} \tag{21}$$

At steady-state $V_C(t) = V_C(t+T)$ and we obtain equation for integration constant B:

$$B = \exp\left(-\frac{T}{\xi}\right)\left\{\frac{1}{\xi}\int_0^T V_0 \sin\omega\theta \exp\left(\frac{\theta}{\xi}\right)d\theta + B\right\} \tag{22}$$

It can be solved as

$$B = \frac{\frac{1}{\xi}\int_0^T V_0 \sin\omega\theta \exp\left(\frac{\theta}{\xi}\right)d\theta}{\exp\left(\frac{T}{\xi}\right)-1} = -\frac{\xi\omega V_0}{1+(\xi\omega)^2} \tag{23}$$

Therefore voltage at the capacitor is

$$\begin{aligned} V_C(t) &= \exp\left(-\frac{t}{\xi}\right)\left\{\frac{1}{\xi}\int_0^t V_0 \sin\omega\theta \exp\left(\frac{\theta}{\xi}\right)d\theta - \frac{\xi\omega V_0}{1+(\xi\omega)^2}\right\} \\ &= V_0\frac{\sin\omega t - \xi\omega\cos\omega t}{1+(\xi\omega)^2} \end{aligned} \tag{24}$$

and current through the capacitor:

$$i_C = C\frac{dV_C}{dt} = CV_0\omega\frac{\cos\omega t + \xi\omega\sin\omega t}{1+(\xi\omega)^2} = \frac{V_0}{R_2}\omega\xi\frac{\cos\omega t + \xi\omega\sin\omega t}{1+(\xi\omega)^2} \tag{25}$$

Total current is:

$$i_{tot} = i_m + i_C \tag{26}$$

Now we consider a few examples how resistance can depend on voltage and find total current. Different voltage gated channels can have different voltammetric characteristics and dependencies of resistance on voltage.

Case 1: linear function

Let the steady state resistance depend on voltage in a linear way (**Fig. 2A**):

$$h(V) = 1 + V/\psi, \tag{27}$$

where ψ is a certain parameter with dimension of voltage, and let voltage change harmonically:

$$V(t) = V_0 \sin\omega t. \tag{28}$$

Here V_0 is the amplitude; ω is the angular frequency and period $T = 2\pi/\omega$. Then from eq. (8) we can find the constant of

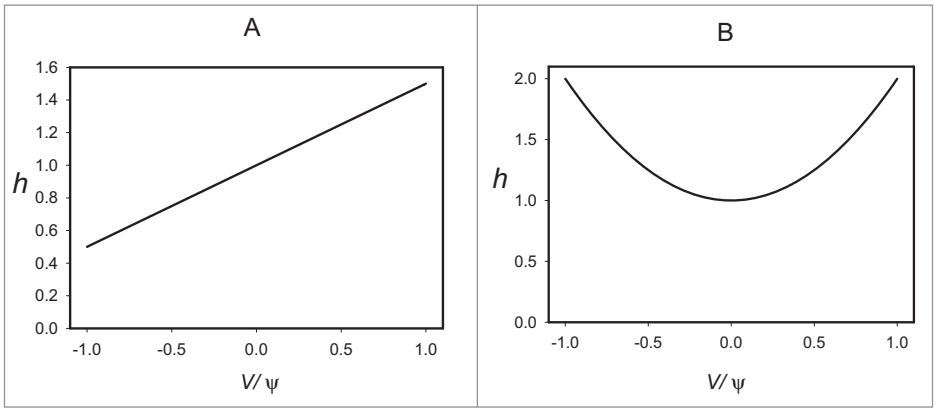

Figure 2. Graphical representation of equations 20 (**A**) and 25 (**B**) for the steady state resistance *h(V)*, which depends on voltage *V* in a linear (**A**) or quadratic (**B**) way.

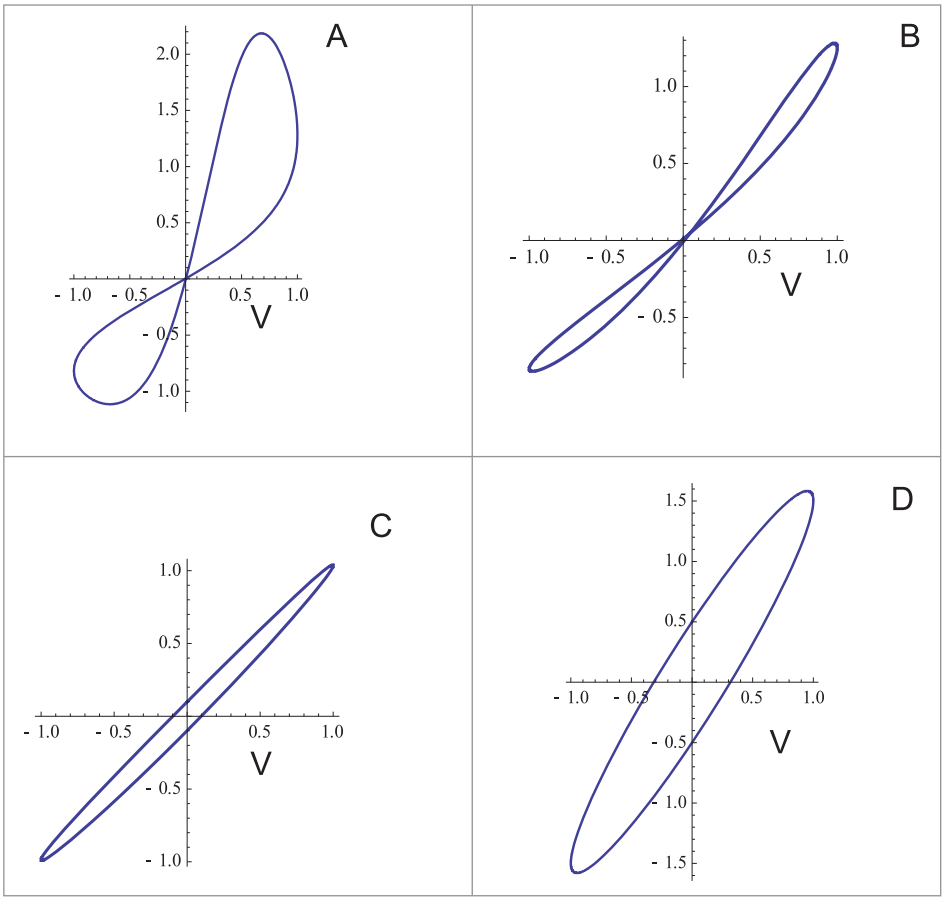

Figure 3. Total electrical current trough a memristor and a capacitor as a function of applied voltage estimated from equations (18, 19 and 24) at different frequencies of a bipolar periodic sinusoidal wave: (**A**) ωτ = 0.3; (**B**) ωτ = 1; (**C**) ωτ = 10, and (**D**) ωτ = 100.

integration A as

$$A = R_0\left[1 - \frac{\tau\omega V_0/\psi}{1+(\tau\omega)^2}\right] \qquad (29)$$

Therefore the resistance changes during the cycle as

$$R(t) = R_0\left\{1 + \frac{a[\sin(t\omega) - \tau\omega\cos(t\omega)]}{1+(\tau\omega)^2}\right\} \qquad (30)$$

and the current through the memristor is

$$i_m(t) = \frac{V(t)}{R(t)} = \frac{V_0\sin(t\omega)}{R_0\left\{1 + \frac{a[\sin(t\omega) - \tau\omega\cos(t\omega)]}{1+(\tau\omega)^2}\right\}} \qquad (31)$$

Now we can plot the total current $i_{tot}(t)$ as a function of voltage $V(t)$. We plot the values at ordinate in units of V_0/R_0 and at abscissa in units of V_0. We have 2 characteristic parameters of time: τ for the branch with memristor and ξ for the branch with capacitor. Comparison with experimental observations suggests that $\tau/\xi = 100$. As was mentioned before, parameter $\tau\omega$ is the normalized frequency which determines characteristic shapes of the curves in the plot of the current as a function of voltage. The most distinguished shapes were found at the following values of this parameter: the *very low frequency* $\omega\tau = 0.3$ (**Fig. 3A**), *low frequency* $\omega\tau = 1$ (**Fig. 3B**), *medium frequency* $\omega\tau = 10$ (**Fig. 3C**), and *high frequency* $\omega\tau = 100$ (**Fig. 3D**).

So at low frequency we have self crossing loop, which transforms into oval at high frequency.

Case 2: quadratic function

Let the steady-state resistance depend on voltage in a quadratic way (**Fig. 2b**):

$$f(V) = 1 + (V/\psi)^2, \qquad (32)$$

where ψ is again a certain parameter with dimension of voltage, and let voltage changes harmonically (Equation 12). Then constant of integration A can be found as

$$A = R_0\left[1 + \frac{2(\tau\omega)^2}{(1+4\tau^2\omega^2)}\left(\frac{V_0}{\psi}\right)^2\right] \qquad (33)$$

and Equation (4) gives for the resistance

$$R_m(t) = R_0\left\{\left[1+\frac{1}{2}\left(\frac{V_0}{\psi}\right)^2\right]-\frac{1}{2}\left(\frac{V_0}{\psi}\right)^2\frac{[\cos(2t\omega)+2\tau\omega\sin(2t\omega)]}{\left[1+4(\tau\omega)^2\right]}\right\} \quad (34)$$

The current flowing through this resistance is

$$i_m(t)=\frac{V(t)}{R(t)}=\frac{V_0\sin(t\omega)}{R_0\left\{\left[1+\frac{1}{2}\left(\frac{V_0}{\psi}\right)^2\right]-\frac{1}{2}\left(\frac{V_0}{\psi}\right)^2\frac{[\cos(2t\omega)+2\tau\omega\sin(2t\omega)]}{\left[1+4(\tau\omega)^2\right]}\right\}} \quad (35)$$

It is interesting to note that though the external voltage changes with frequency ω, the resistance R_m changes with double frequency 2ω (Equation 14). The current through the memristor i_m contains components with both primary ω and double frequency $2\,\omega$ (Equation 15).

Now we can plot the total current as a function of voltage (**Fig. 4**). For certainty we select the following value of the parameter $\frac{1}{2}\left(\frac{V_0}{\psi}\right)^2=1$. Once again we plot the values at ordinate in units of V_0/R_0 and at abscissa in units of V_0. We have 2 characteristic parameters of time: τ for the branch with memristor and ξ for the branch with capacitor. Comparison with experimental observations suggests that $\tau/\xi=100$. As was mentioned before, parameter τω is the normalized frequency which determines characteristic shapes of the curves in the plot of the current as a function of voltage. The most distinguished shapes were found at the following values of this parameter: it is *very low frequency* $\omega\tau=0.01$(**Fig. 4A**), *low frequency* $\omega\tau=0.1$ (**Fig. 4B**), *medium frequency* $\omega\tau=1$(**Fig. 4C**), and *high frequency* $\omega\tau=10$ (**Fig. 4D**).

At very low frequency we have a line (no loop), at low and medium frequency we have a pinched loop at the origin without crossing, and at high frequency we have an oval without pinching. This transformation occurs due to the presence of the capacitor in parallel with a memristor.

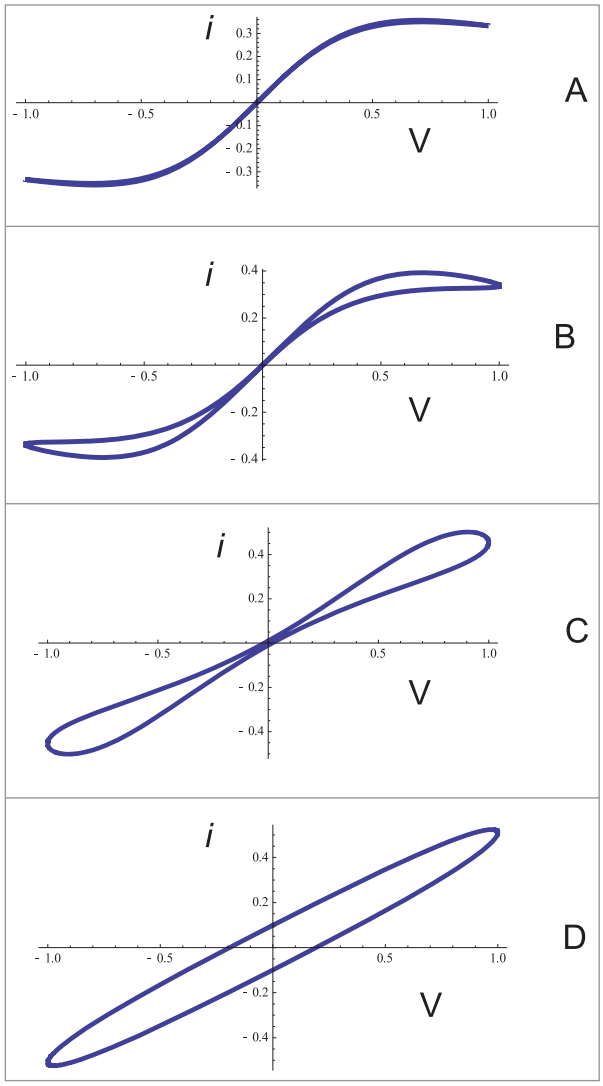

Figure 4. Total electrical current trough a memristor and a capacitor as a function of applied voltage estimated from equations (18, 19 and 28) at different frequencies of a bipolar periodic sinusoidal wave: (**A**) ωτ = 0.01; (**B**) ωτ = 0.1; (**C**) ωτ = 1, and (**D**) ωτ = 10.

Experimental

Bipolar sinusoidal or triangle periodic waves with amplitude V_{FG} were applied from a function generator (**Fig. 5**). To measure electrical current we included in the circuit additional resistor R, so that electrical current was found as $I = V_R/R$. Potential difference, V_P, between electrodes in plants is equal to $V_P = V_{FG} - V_R$. V_P is always less than V_{FG} because of a voltage drop on a resistor R.

Cyclic voltammetry in **Figure 6** shows how electrical current depends on voltage induced by bipolar sinusoidal wave at different frequencies when platinum electrodes inserted across the pulvinus of the *Mimosa pudica*. At low frequencies of scanning, the plot displays a common pinched point with self-crossing between curves (**Fig. 6A**). The common pinched point disappears at high frequencies 1 kHz (**Fig. 6B**) and memristor transforms to a resistor. For a plant tissue, the pinched hysteresis loop transforms to a non-pinched hysteresis loop instead of a single line $I = V/R$ at high frequencies of the applied voltage because according to Equation (18) the amplitude of electrical current depends also on capacitance of a plant tissue and electrodes, frequency and direction of scanning. **Fig. 6B** shows the capacitance currents in cathodic and anodic lines. The loop in **Fig. 6B** at 1 kHz shows that there is a linear capacitor in parallel with the memristor seen at low frequencies (**Fig. 6A**) where the capacitor effect is negligible. If we use instead of a plant tissue any resistor, the *I-V* curve will become a straight line with a single-valued curve without a loop. **Fig. 6** shows the curves for 4 different frequencies. They demonstrate the same variation of curves with change of frequency: at low frequency the loop appears, and the curve transforms into oval at high frequencies.

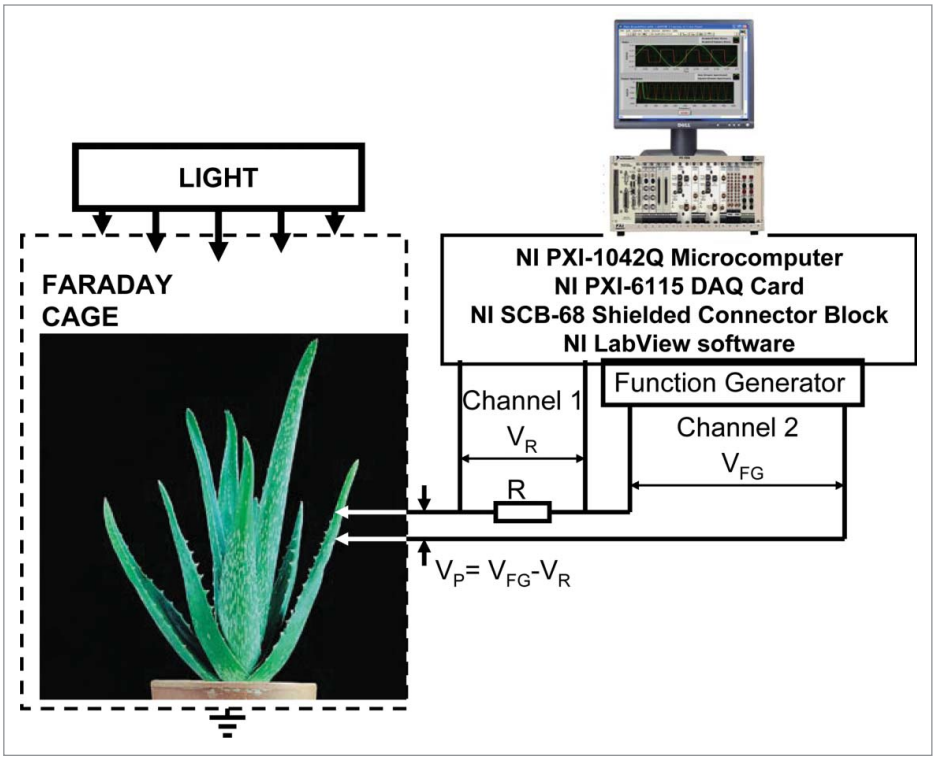

Figure 5. Block diagram of the data acquisition and electrostimulation system.

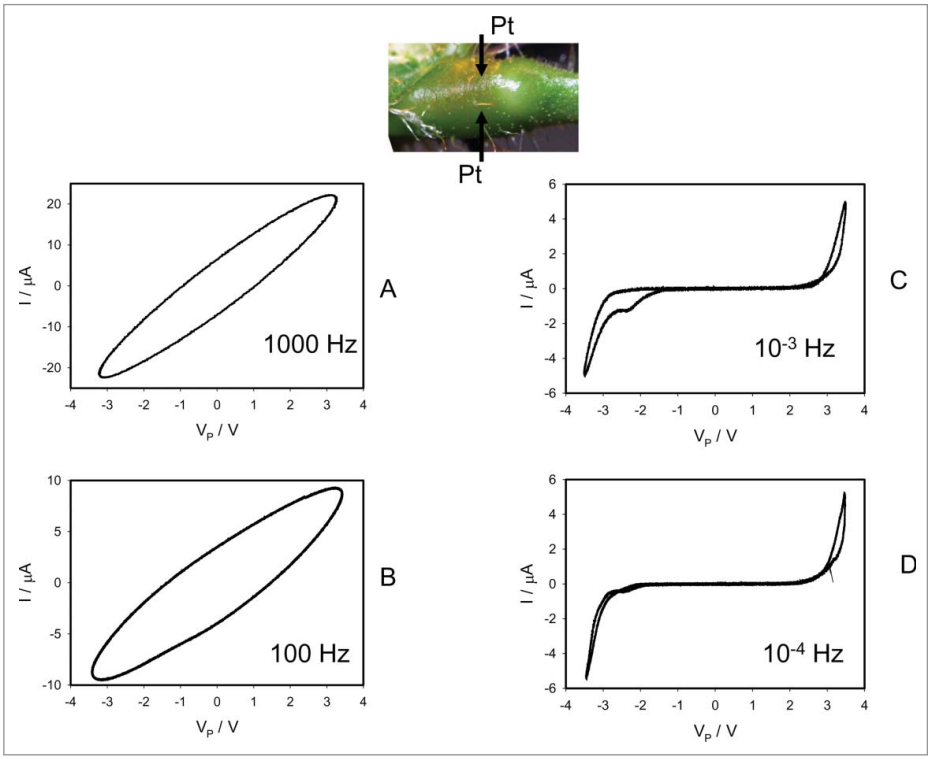

Figure 6. Electrical current *I* versus voltage V_P applied across a pulvinus of *Mimosa pudica* plant. Frequency of periodic bipolar sinusoidal voltage scanning was 1000 Hz (**A**), 100 Hz (**B**), 0.001 Hz (**C**) and 0.0001 Hz (**D**). Position of Pt electrodes in the pulvinus of *Mimosa pudica* is shown. These results were reproduced 16 times.

Figure 7 shows the effect of TEACl on electrical current induced by bipolar sinusoidal wave when platinum electrodes inserted along the pulvinus of *Mimosa pudica*. The pinched hysteresis loop (**Fig. 6**) disappears and the memristive system transforms to a resistance. Frequency of sinusoidal voltage scanning was 0.001 Hz. Panel A in **Figure** 7 shows responses to bipolar periodic electrostimulating waves with frequency of 10^{-3} Hz and panels B corresponds to responses to waves with frequencies of 1000 Hz.

TEACl decreases the amplitude of electrical current between electrodes in pulvinus of the *Mimosa pudica*. TEACl is known as a blocker of voltage gated potassium channels. Tetraethylammonium chloride, an inhibitor of voltage gated K^+ channels transforms a memristor to a conventional resistor in plant tissue. Our results demonstrate that a voltage gated K^+ channel in the excitable tissue of plants has properties of a memristor.

Cyclic voltammogram in **Figure 8** shows how electrical current depends on the voltage V_p between electrodes in a leaf of the *Aloe vera* induced by bipolar sinusoidal wave from a function generator with frequency of 0.001 Hz, when platinum electrodes are inserted along the vascular bundles in a leaf of *Aloe vera*. There is a self-crossing between curves and a pinched point in hysteresis loop at low frequency of sinusoidal wave in the voltage-current plane when $I = 0$ μA and $V_P = 0$ V, which is a typical sign of a memristor of a first kind (**Fig. 8A**). In some experiments there is a pinched point in the hysteresis loop at low frequency of sinusoidal wave in the voltage-current plane when $I = 0$ μA and $V_P = 0$ V without a self-crossing between curves, which is a typical sign of a memristor of a second kind. Increasing of a sinusoidal wave frequency to 1000 Hz leads to the disappearing of a pinched point in the complete agreement with characteristics of memristors, which had a small "parasitic" capacitor connected across the memristor. This capacitance can be a function of membrane, electrodes and plant tissue capacitances. We found that

a self-crossing between curves exists in 71% of experiments (Mean 71.43%, Std. Dec. 46.88%, Std. Err. 12.53%, n = 14). The amplitude of electrical current increases with an increase of applied voltage amplitude to the leaf of *Aloe vera*.

Discussion

We presented here a very simple model of a resistor which properties depend on voltage and analyzed its reaction to periodically changing electrical voltage. This reaction strongly depends on the frequency of the applied voltage. At low frequency, the current voltage characteristic exhibits a typical pinched hysteresis curve.

The memristor driven by the sinusoidal current generates *I-V* pinched hysteresis loops in cyclic voltammograms. The pinched hysteresis loop is a double-valued Lissajous figure of ($V(t)$, $I(t)$) for all times t, except when it passes through the origin, where the loop is pinched. It was theoretically shown that the voltage gated potassium ion channels in axons are locally-active memristors.[11-14] Voltage-gated ionic channels control the plasma membrane potential and the movement of ions across membranes thereby regulating various biological functions.[25-29] These biological nanodevices play vital roles in signal transduction in higher plants. Propagation of action potentials in plants is documented in literature. TEACl, an inhibitor of voltage gated K^+ channels, transform a memristor to a resistor.[15,30,31] Plants have these voltage gated potassium ion channels associated with plasma membranes.[16]

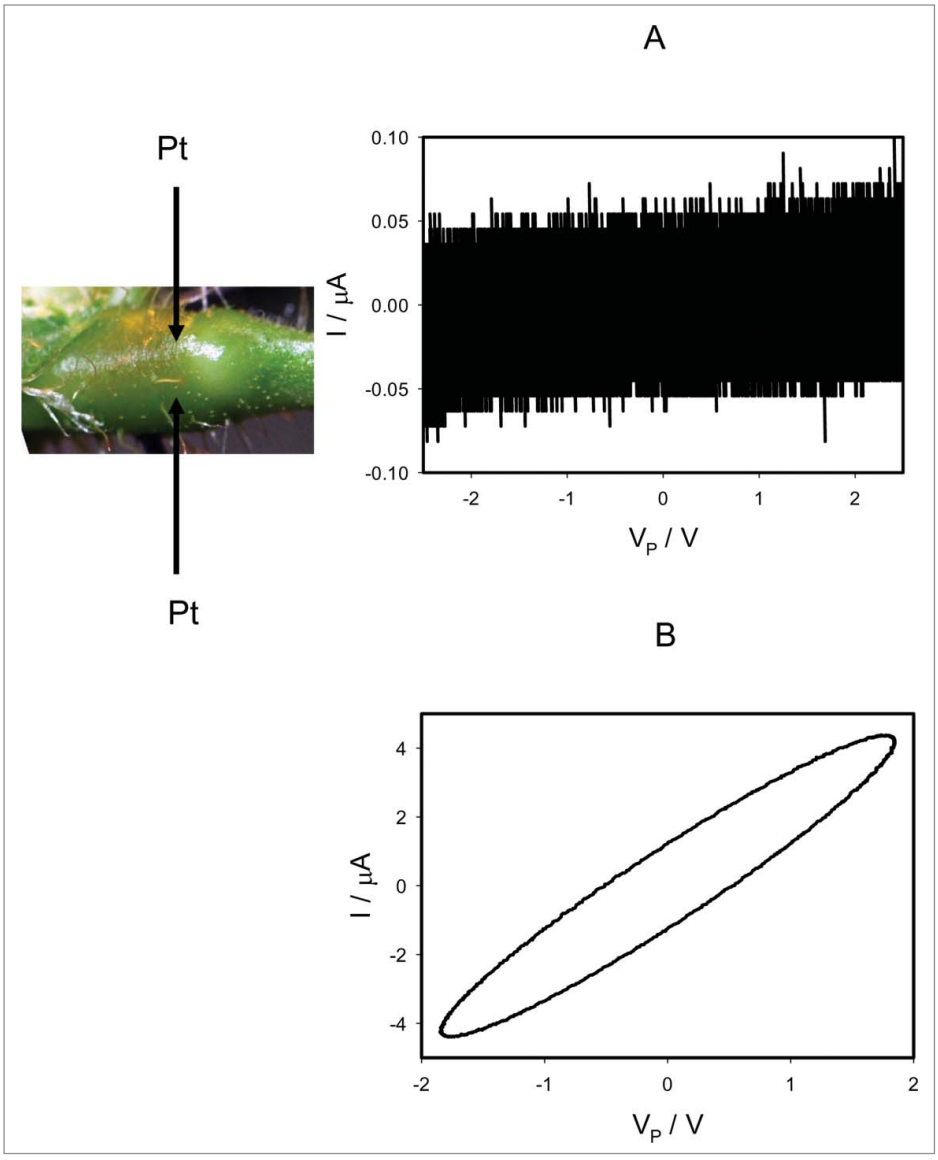

Figure 7. Cyclic voltammetry along a pulvinus after injection of 0.05 mL of 10 mM TEACl in a stem above and below of the pulvinus 5 hours before electrical measurements. Frequency of sinusoidal voltage scanning was 0.001 Hz (**A**) or 1000 Hz (**B**). Position of Pt electrodes in the pulvinus of *Mimosa pudica* are shown.

Our analytical model of a memristor in plants with a capacitor connected in parallel shows that at very high frequencies instead of a single-valued function of a memristor (**Fig. 4C and D**) there are 2 cathodic and anodic lines in voltammetric diagrams (**Fig. 6A, 6B and 7B**). The pinched hysteresis loop of memory elements, when subject to a periodic stimulus, can be self crossing (type I memristor) or not (type II memristor).

Cyclic voltammograms in **Figures 6 and 8** show memristive properties of the *Mimosa pudica* pulvinus and *Aloe vera* leaf. The electrophysiology of plants should include memristors as essential model building blocks in electrical networks. The memristor is an "ideal" circuit element, and in plant tissue memristors coexist with membrane capacitors.

Materials and Methods

Plants

The seeds of *Mimosa pudica L.* were soaked in warm water (30°C) for 48 h. They were then grown in well drained peat moss at 21°C with a 12:12 hr light:dark photoperiod. After growing for 2 weeks, the seedlings were transplanted into pots and placed inside a plant growing chamber. The plants were

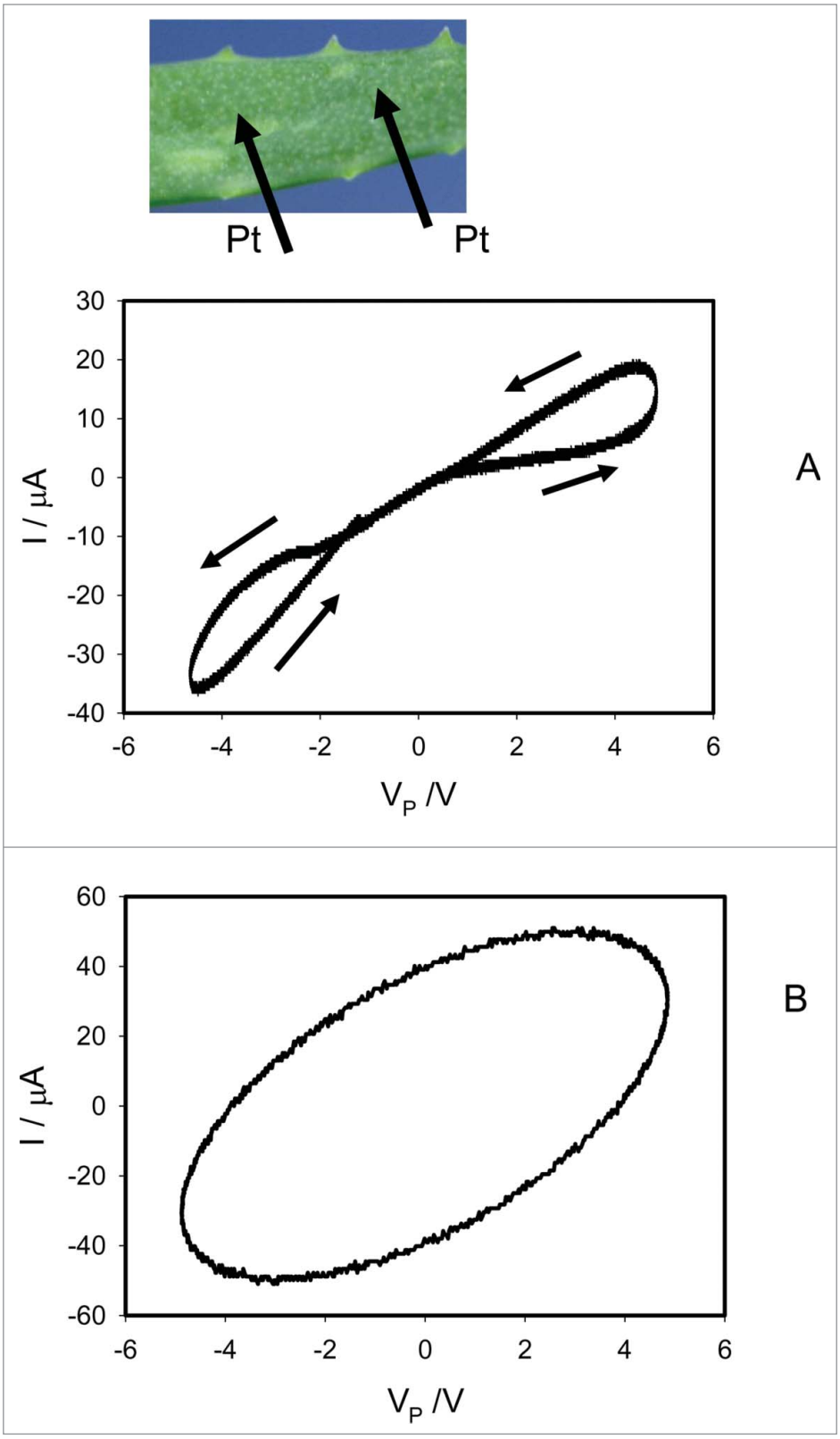

Figure 8. Cyclic voltammetry of a leaf of *Aloe vera*. Frequency of periodic bipolar sinusoidal voltage scanning was 0.001 Hz (**A**) and 1000 Hz (**B**). Position of Pt electrodes in a leaf of *Aloe vera* is shown. These results were reproduced 16 times.

watered every day. Two-3 month old plants were used for the experiments.

Fifty *Aloe vera* L plants were grown in clay pots. *Aloe vera* plants had 25–35 cm leaves.

Irradiance was 700–800 µmol photons $m^{-2}s^{-1}$. The humidity averaged 45–50%. All experiments were performed on healthy adult specimens.

Chemicals

Tetraethylammonium chloride (TEACl) was obtained from *Fluka* (*New York, NY, USA*).

Electrodes for Extracellular Measurements

Platinum electrodes were prepared from Teflon coated platinum wires (A-M Systems, Inc., Sequim, WA, USA) with diameter of 0.076 mm. In all experiments we used identical Pt electrodes as a measuring and as reference (*Ref*) electrodes.

Data Acquisition

All measurements were conducted in the laboratory at constant room temperature of 22°C inside a Faraday cage which was mounted on a vibration-stabilized table (**Fig. 5**). High speed data acquisition of low-pass filtered signals was performed using microcomputer NI-PXI-1042Q *(National Instruments, Austin, TX, USA*) with simultaneous multifunction I/O plug-in data acquisition board NI-PXI-6115 *(National Instruments*) interfaced through a NI SCB-68 shielded connector block to electrodes.

Plant Electrostimulation

The function generator FG300 (*Yokagawa, Japan*) was interfaced to NI-PXI-1042Q microcomputer and used for electrostimulation of plants. We selected a resistor $R = 10$ kω for measuring of voltage, V_R, for estimation of electrical current I.

Statistics

All experimental results were reproduced 25 times on different plants. Software SigmaPlot 12 (Systat Software, Inc., San Jose, CA, USA) was used for statistical analysis of experimental data.

Disclosure of Potential Conflicts of Interest

No potential conflicts of interest were disclosed.

Funding

This article is based upon work supported in part by the National Science Foundation under grant number CBET-1064160 and in part by the U. S. Army Research Office under contract/grant number W911NF-11–1–0132 to AG Volkov. L Chua's research is supported in part by AFOSR grant number FA9550–13–1–0136 and an EC Marie-Curie Fellowship.

References

1. Chua L. Memristor - The missing circuit element. IEE Trans Circuit Theory 1971; 18:507-19; http://dx.doi.org/10.1109/TCT.1971.1083337
2. Strukov DB, Snider GS, Stewart DR, Williams RS. The missing memristor found. Nature 2008; 453:80-3; PMID:18451858; http://dx.doi.org/10.1038/nature06932
3. Borghetti J, Sinder GS, Kuekes PJ, Yang JJ, Stewart DR, Williams RS. Memristive switches enable stateful logic operations via material implication. Nature 2010; 464:873-876; PMID:20376145; http://dx.doi.org/10.1038/nature08940
4. Chua L. Resistance switching memories are memristors. Appl Phys A 2011; 102:765-83; http://dx.doi.org/10.1007/s00339-011-6264-9
5. Jo SH, Chang T, Ebong I., Bhadviya BB, Mazumder P, Lu W. Nanoscale memristor device as synapse in neuromorphing systems. Nano Lett 2010; 10:1297-1301; PMID:20192230; http://dx.doi.org/10.1021/nl904092h
6. MacVittie K, Katz E. Electrochemical systems with memimpedance properties. J Phys Chem C 2013; 117:24943-24947; http://dx.doi.org/10.1021/jp409257v
7. MacVittie K, Katz E. Self-powered electrochemical memristor based on a biofuel cell - towards memristors integrated with biocomputing systems. Chem Commun 2014; 50:4816-4819; http://dx.doi.org/10.1039/c4cc01540a
8. Pershin YV, La Fontaine S, Di Ventra M. Memristive model of amoeba learning. Phys Rev E 2009; 80:021926.0; http://dx.doi.org/10.1103/PhysRevE.80.021926
9. Smerieri A, Berzina T, Erokhin V, Fontana MP. Polymeric electrochemical elements for adaptive networks: Pulse mode. J Appli Phys 2008; 104:114513-8; http://dx.doi.org/10.1063/1.3033399
10. Adhikaru AP, Sah MPd, Kim H, Chua L. The fingerprints of memristor. IEEE Trans Circuits Systems 2013; http://dx.doi.org/10.1109/TCSI.2013.325671
11. Chua L, Sbitnev V, Kim H. Hodgkin-Huxlew axon is made of memristors. Internat J Bifurcation Chaos 2012; 22:1230011-1-48; http://dx.doi.org/10.1142/S021812741230011X
12. Chua L, Sbitnev V, Kim H. Neurons are poised near the edge of chaos. Internat J Bifurcation Chaos 2012; 22:1250098-1-49; http://dx.doi.org/10.1142/S0218127412500988
13. Chua L. Memristor, Hodgkin-Huxley, and Edge of Chaos. Nanotechnology 2013; 24:383001; PMID:23999613; http://dx.doi.org/10.1088/0957-4484/24/38/383001
14. Sah M, Kim H, Chua L. Brains are made of memristors. IEEE Circuits Systems 2014; 14:12-36; http://dx.doi.org/10.1109/MCAS.2013.2296414
15. Volkov AG, Tucket C, Reedus J, Volkova M, Markin VS, Chua L. Memristors in plants. Plant Signal Behav 2014; 9:e28152.
16. Hedrich R. Ion channels in plants. Physiol Rev 2012; 92:1777-1811; PMID:23073631; http://dx.doi.org/10.1152/physrev.00038.2011
17. Arabidopsis Genome Iniciative. Analysis of the genome sequence of the flowering plant *Arabidopsis thaliana*. Nature 2000; 408:796-815; PMID:11130711; http://dx.doi.org/10.1038/35048692
18. Ward JM, Maser P, Schroeder J. Plant ion channels: gene families, physiology, functional genomics analyses. Ann Rev Physiol 2009; 71:59-82; http://dx.doi.org/10.1146/annurev.physiol.010908.163204
19. Williams RS, Pickett MD, Strachan JP. Physics-based memristor models. 2013 IEEE Int Sym Circuits and Systems (ISCAS) 2013; pp.217-220; http://dx.doi.org/10.1109/ISCAS.2013.6571821
20. Itoh M, Chua L. Duality of memristor circuit. Internat J Bifurcation Chaos 2013; 23:1330001-1-50; http://dx.doi.org/10.1142/S0218127413300012
21. Elgabra H, Farhat IAH, Hosani ASA, Homouz D, Mohammad B. Mathematical modeling of a memristor device. Inte Conf Innov Inform Technol 2012; p.156-161; http://dx.doi.org/10.1109/INNOVATIONS.2012.6207722
22. Ascoli A, Corinto F, Senger V, Tetzlaff R. Memristor model comparison. IEEE Circuits Systems Mag 2013; 13:89-105; http://dx.doi.org/10.1109/MCAS.2013.2256272
23. Kvatinsky S, Friedman EG, Kolodny A, Weiser UC. Team-threshold adaptive memristor model. IEEE Trans Circuits Systems 2013; 60:211-221; http://dx.doi.org/10.1109/TCSI.2012.2215714
24. Biolek D, Biolek Z, Biolkova V. Interpreting area of pinched memristor hysteresis loop. Electronics Lett 2014 50:74-5; http://dx.doi.org/10.1049/el.2013.3108
25. Volkov AG, Foster JC, Ashby TA, Walker RK, Johnson JJ, Markin VS. *Mimosa pudica*: Electrical and mechanical stimulation of plant movements. Plant Cell Environm 2010; 33:163-173; http://dx.doi.org/10.1111/j.1365-3040.2009.02066.x
26. Volkov AG, Foster JC, Jovanov E, Markin VS. Anisotropy and nonlinear properties of electrochemical circuits in leaves of *Aloe vera* L. Bioelectrochem 2011; 81 4-9; http://dx.doi.org/10.1016/j.bioelechem.2010.11.001
27. Volkov AG, Foster JC, Jovanov E, Markin VS. Anisotropy and nonlinear properties of electrochemical circuits in leaves of *Aloe vera* L. Bioelectrochem 2011; 81:4-9; http://dx.doi.org/10.1016/j.bioelechem.2010.11.001
28. Volkov AG, O'Neal L, Volkova MI, Markin VS. Morphing structures and signal transduction in *Mimosa pudica* L. induced by localized thermal stress. J Plant Physiol 2013;170:1317-27; PMID:23747058; http://dx.doi.org/10.1016/j.jplph.2013.05.003
29. Markin VS, Volkov AG. Morphing structures in the Venus flytrap. In: Volkov AG, editor. Plant Electrophysiology. Signaling and Responses. Berlin: Springer; 2012. p. One-31.
30. Volkov AG, Tucket C, Reedus J, Mitchell CM, Volkova M, Markin VS, Chua L. Memristors in the Venus flytrap. Plant Signal Behav 2014; 9:e29204-1-12; PMID:24837439; http://dx.doi.org/10.4161/psb.29204
31. Volkov AG, Reedus J, Mitchell CM, Tucket C, Forde-Tucket V, Volkova M, Markin VS, Chua L. Memristors in the electrical network of *Aloe vera* L. Plant Signal Behav 2014; 9:e29056-1-7; PMID:24806097; http://dx.doi.org/10.4161/psb.29056